

Evaluating Visual Variables in a Virtual Reality Environment

Somnath Arjun, G S Rajshekar Reddy, Abhishek Mukhopadhyay, Sanjana Vinod, Pradipta Biswas
I³D Lab, Indian Institute of Science
Bangalore 560012, India
{somnatharjun, rajshekarg, abhishekmukh, sanjanam, pradipta}@iisc.ac.in

Large amount of multi-dimensional data can be difficult to visualize in standard 2D display. Virtual Reality and the associated 3rd dimension may be useful for data analysis; however, 3D charts may often be confusing to users rather conveying information. This paper investigated and evaluated graphical primitives of 3D charts in a Virtual Reality (VR) environment. We compared six different 3D graphs involving two graph types and five visual variables. We analysed ocular and EEG parameters of users while they undertook representative data interpretation tasks using 3D graphs. Our analysis found significant differences in fixation rate, alpha and low-beta EEG bands among different graphs and a bar chart using different sizes of columns for different data values found to be preferred among users in terms of correct response. We also found that colour makes it easier to interpret nominal data as compared to shape and size variable reduces the time required for processing numerical data as compared to orientation or opacity. Our results can be used to develop 3D sensor dashboard and visualization techniques for VR environments.

Evaluation. Visual variables. Visualization. Virtual Reality. Eye Tracking. Cognitive load.

1. Introduction

Analysing data is turning increasingly difficult as the size and complexity of datasets continue to grow every day. Using visualisation techniques for data analysis is a popular method because it exploits the human visual system as a means of communication for interpreting information. In recent times, a plethora of visualisation techniques have been developed to explore large and complex data. The rise of visualisation techniques has made the practice of evaluation of visualization techniques even more critical. A number of empirical evaluation methods for visualisation techniques have been developed in the last two decades. There has been a steady increase in evaluation methods those include human participants' performances and subjective feedback. Isenberg et al. [1] divided evaluation methods into eight categories. They reported that Qualitative Result Inspection, Algorithmic Performance, User Experience and User Performance are the most common evaluation scenarios. In this paper, we have evaluated 3D visualisation in a VR environment by comparing user performance and experience across six types of visualisation techniques. We have investigated and compared visualisations using ocular parameters and EEG (Electroencephalogram). Ocular parameters are already extensively used to explain and model visual perception [39], analyse cognitive

load [18, 20, 21] and areas of interest in complex visual stimuli [22, 23]. Comparison of 2D graphs used for representing quantitative data using eye tracking device has been undertaken for evaluating user/task characteristics and finding appropriate graphs [2,3]. Drogemuller et al. [42] evaluated navigation techniques for 3D graph visualisations in VR environment. Ware and Mitchell [33] studied graph visualisation in 3D, specifically they compared 3D tubes with 2D lines to display the links in a graph. They reported that with motion and stereoscopic depth cues, skilled observers could identify paths in a 1000-node graph with an error rate less than 10% compared to 28% with 2D graphs. Although tools and techniques have been developed in a VR environment for exploring and interacting with graphs effortlessly [4,5,6], researchers have hardly explored studies that compare 3D graphs. A comparative survey of user experiences with 3D charts in a VR environment was undertaken in [7,8]. However, these studies were primarily limited to a single graph.

Visualisation can be termed as a collection of graphical objects. Ward et al. [9] state that there are eight ways in which graphical objects can encode information, i.e., eight visual variables – position, shape, size, opacity, colour, orientation, texture, and motion. These eight variables can be adjusted as necessary to maximise the effectiveness of a visualisation to convey information. Garlandini and

Fabrikant [35] explored the effectiveness and efficiency of these visual variables in 2D cartography. Their results revealed that the variable size was most effective and efficient in guiding viewers, and orientation played the least role. However, researchers have not investigated and compared visual variables in 3D graphs previously. We consider the problem of comparing visual variables of 3D graphs for representing 1D numerical data. In particular, we compare variables that are used to depict numerical data - size, orientation and opacity and nominal data - colour and shape. Somnath [3] compared 2D graphs and reported that users are more comfortable using bar and area charts than line and radar charts. Extending the work in the VR environment, we also compare the 3D bar chart and area chart to find if there is any difference between them in the VR environment. The readers may be interested in knowing:

1. Which 3D graph is best in terms of correct data interpretation?
2. Which visual variable(s) is (are) easier to interpret than others?
3. Does the 3rd dimension add a value?
4. Are there differences among graph types with respect to-?
 - a. Ocular parameters and
 - b. Cognitive load while interpreting graphs.

The paper is organised as follows. We discuss the related work in Section 2 followed by user study in Section 3. Methodology is discussed in Section 4, analysis and results are discussed in Section 5 followed by discussion in Section 6. We have presented concluding remarks in Section 7.

2. Related Work

Visualisation is defined as the communication of information using graphical representations. Graphics related application demands in depth understanding of graphics primitives and their properties to communicate information. In total, there are eight ways in which graphical objects can encode information [9]. Variables such as size, orientation, and opacity [9, 36] encode quantitative data information, while colour and shape are used for visualising nominal data. Fisher et al. [34] investigated which 3D graph type was easiest to interpret among bar, pie, floating line, mixed bar/line, and layered line charts. It was revealed that information extracted from bar and pie charts were found to be more effective than others. Additionally, it was found that the participants had better information retention with pie charts than bar charts. Hitherto, researchers have either developed new

methods or discussed in detail how specific approaches need to be extended for visualisation evaluation. Evaluation of visualisation is primarily based on empirical methods. In particular, empirical evaluation and the consideration of human factors are discussed in [10,11,12]. Isenberg et al. [1] identified eight evaluation scenarios. They reported that Qualitative Result Inspection (QRI), Algorithmic Performance (AP), User Experience (UE) and User Performance (UP) to be the most common evaluation scenarios. In User Performance evaluation, Livingston et al. [13] focused on time taken and errors committed to complete a task using a new technique [13]. It was found that a large number of UP studies were done with 10-15 participants [1]. Evaluation of visualisation using an eye-tracking device [3] is an example of a UP evaluation scenario. Understanding user performances and feedback includes tasks where the user must answer a set of questions after assessing the visualisation techniques [2,3]. A set of low-level analysis tasks that capture user's activities while employing visualisation for understanding data was presented in [14]. We have adopted four out of these ten analytical task questions [14] for our user study.

Cognitive measures also have an influence on a user's performance and satisfaction while working with visualisations [15, 16, 17]. Peck et al. [32] utilized fNIRS to examine how participants process bar graphs and pie charts, and cognitive loads associated with them. Their results indicated that there was no significant difference among bar graph and pie chart, and this result also correlated with the results of the NASA TLX questionnaire. Furthermore, psychologists [19] have reported a strong association between cognitive load and pupil dilation of eyes. Marshall [20] proposed a wavelet-based algorithm to detect a hike in pupil dilation corresponding to an increase in cognitive load. Gavas [21] and Duchowski [22] also estimated cognitive load from pupil dilation. Saccadic Intrusion, change in fixation duration, and blink count [23] are also used for measuring cognitive load. Prabhakar et al. [18] investigated the efficacy of various ocular parameters to estimate cognitive load and detect driver's cognitive state. They derived gaze and pupil-based metrics and proposed a machine learning model classifying different levels of cognitive states. The use of ocular parameters has also shown an impact on evaluating visualisation performance [3,30,31]. A comparative study on user experiences with 3D graphs in VR environments was undertaken in [7,8]. There are no studies reported in literature which considers ocular parameters while the user observes different visualisation techniques in a VR environment. Gaze fixations are used for identifying areas of interest in graphs [3]. Research has been conducted on identifying user gaze differences for alternative visualisations [24], task types [25] or

individual user differences [26]. In [24], linear and radial versions of bar, line, area, and scatter graphs were evaluated in terms of the cognitive load induced. It was revealed that participants took more time to complete tasks with the radial versions than their linear counterparts. It was also concluded that radial graphs are most useful for finding extreme values. In this work, we investigated ocular parameters like fixation rate, saccade rate and revisit sequences while users undertake tasks in VR environment. We also investigated pupil dilation and EEG data to estimate cognitive load of participants.

3. User study

In order to investigate and compare visual variables and charts, we designed and conducted a user study with six types of visualisation techniques. Each technique displayed numerical data and nominal data using different combinations of visual variables. We considered synthetic sensor data in our study and used five different sensors: temperature, humidity, smoke, air, and light. We have three instances of each sensor, and we use the term “node” to refer to all instances of a particular type of sensor. The data type of node was nominal. In total, there are 15 data points and 5 sensor nodes. The six visualisation techniques are explained next.

3.1 Visualisation charts

We developed and used six types of charts in our study, bar-size/bar chart (BC), bar-orientation (BOR), bar-opacity (BO), shape-size (SS), shape-opacity (SO) and area chart (AC). Nodes were arranged on the x-axis and instances of each node were arranged in the z-axis for all six charts. The representation of node and real valued sensor for each chart are described next.

3.1.1. Bar-Size chart

In this technique, the nodes are represented by different colours, and the size of bars depicts a numerical value, as shown in Figure 1. The size of bars is scaled along the y-axis. The scaled value of sensor is computed using -

$$SV_{Sensor} = \frac{RV_{Sensor} - S_{Min}}{S_{Max} - S_{Min}} * 10,$$

where SV_{Sensor} is the scaled value of sensor (length of the bar), RV_{Sensor} is the real value of sensor, S_{Min} is the minimum value of the sensor and S_{Max} is the maximum value of the sensor.

3.1.2. Bar-Orientation chart

As before nodes are represented by different colours but numerical values of sensors are defined by the orientation of bars. Bars are oriented or

rotated along the x-axis to display values of sensors. The rotation is computed using -

$$SV_{Sensor} = \left(\frac{RV_{Sensor} - S_{Min}}{S_{Max} - S_{Min}} * 180 \right) - 90,$$

where SV_{Sensor} is the scaled value of the sensor (rotation of the bar), RV_{Sensor} is the real value of the sensor, S_{Min} and S_{Max} were defined as before.

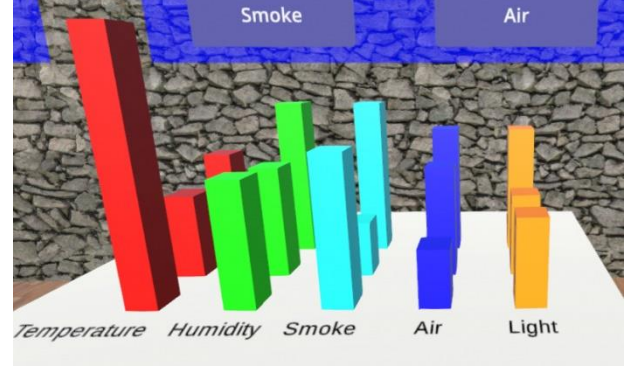


Figure 1: Bar-Size chart

3.1.3. Bar-Opacity chart

Nodes are represented by the unique bar colours, and the opacity of bars is directly proportional to the numerical value of sensors. The darker the bars, the more its value. The real value of the sensor is mapped to the opacity of the bar using the following equation -

$$SV_{Sensor} = \frac{RV_{Sensor} - S_{Min}}{S_{Max} - S_{Min}} * 255,$$

where SV_{Sensor} is the scaled value of sensor (opacity of bar), RV_{Sensor} is real value of sensor, S_{Min} and S_{Max} were defined as before.

3.1.4. Shape-Size chart

This visualisation technique uses a combination of shape and colour to define a node. The numerical values of the sensors are represented by the volume of the shape. The relation between sensor values and scaled values in VR environment follows the equation given below.

$$SV_{Sensor} = \frac{RV_{Sensor} - S_{Min}}{S_{Max} - S_{Min}} * 10,$$

where SV_{Sensor} is scaled value of sensor (size of shape), RV_{Sensor} is real value of sensor, S_{Min} and S_{Max} were defined as before.

3.1.5. Shape-Opacity chart

In this technique, nodes are represented by a combination of shape and colour. Numerical values are defined by the opacity of the shape, as shown in Figure 2. The real value of the sensor is mapped to the opacity of the bar using the following equation.

$$SV_{Sensor} = \frac{RV_{Sensor} - S_{Min}}{S_{Max} - S_{Min}} * 255,$$

where SV_{Sensor} is scaled value of sensor (opacity of shape), RV_{Sensor} is real value of sensor, S_{Min} and S_{Max} were defined as before.

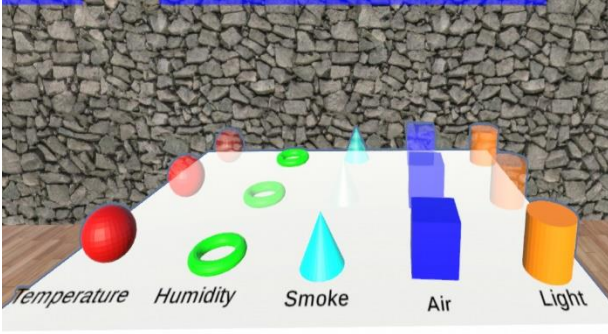


Figure 2: Shape-Opacity chart

3.1.6. Area chart

Sensors are represented by planes in the chart and each sensor has a unique colour. The values of sensors are depicted by the peaks of planes. Each plane is scaled along the y-axis. Relation between sensor value and peak of the plane is given by the following equation.

$$SV_{Sensor} = \frac{RV_{Sensor} - S_{Min}}{S_{Max} - S_{Min}} * 10.$$

3.2 Materials

We used HTC Vive Pro Eye [37] with an inbuilt eye-tracker and refresh rate of 90Hz to collect gaze-based data and pupil diameter (accuracy 0.5° of visual angle). We have also used Emotiv Insight EEG tracker [38] with 5 dry electrodes and sampling rate of 128 Samples per Second (SPS) to collect EEG data. Our computer architecture consists of an Intel Core i5 processor and Nvidia 2070 graphics card.

3.3 Participants

We collected data from 17 participants with an average age of 28 years (male:15 and female: 2) recruited from our university. We took appropriate ethical approval from university ethics committee for conducting the experiment. Participants were tested for visual acuity and all had 20/20 vision.

3.4 Design

We designed and set up a VR environment scene using the Unity 3D game engine. The scene consists of a visualisation chart and a set of 4

questions. The VR scene is shown in Figure 3. We set questions based on low-level tasks by Amar et al. [14]. The four questions that participants were requested to answer are explained below.

Q1: Which node has the highest range?

Participants were asked to compare ranges of five sensor nodes and report the highest value among them.

Q2: Find the node with the maximum and minimum average values?

Participants were first asked to guess the average value of each sensor node across its three instances. From these five estimated average values of five sensor nodes, participants were requested to report the sensor node with the maximum and minimum value. The process involves first browsing through y and z-axes to guess average and then comparison across x-axis.

Q3: Which sensor has its average value nearest to humidity sensor?

Participants were asked to approximate the average value of each sensor as before. We then requested them to report the sensor node whose average value is closest to the average value of the humidity sensor.

Q4: Sort the average values of sensors in descending order.

After estimating each sensor's average value as before, participants were asked to sort those values in descending order.

For example, in Figure 1, the temperature sensor has the highest difference between the maximum and the minimum value (range). After estimating the average value of all sensors, we can notice that the temperature sensor has the maximum average value, and the smoke sensor has the minimum average value. The air sensor's average value is closest to the average value of the humidity sensor. It may be noted that although sensors measure different physical variables, but their values were normalized in the rendering.



Figure 3: Virtual Reality scene

3.5. Procedure

Initially, participants were tested for their visual acuity and allowed the trial if they had 20/20 vision. Then they were briefed about the aim of the study and shown a virtual walkthrough of the environment. We calibrated the hand controller and eye tracker for each participant separately and proceeded with the trail when they could select the target, and the proprietary eye-tracking software indicated the calibration to be successful. We instructed participants to use the VR headset for ten minutes to get accustomed to the VR scene. Participants were instructed to move around the scene using a teleport button on the VR hand controller. When participants were comfortable with the scene, we asked them to start the task by wearing both EEG tracker and HTC Vive Pro Eye. Participants were then requested to observe the visualisation chart and answer four questions.

4. Analysis methodology

This section describes different algorithms used for calculating gaze-based metrics and cognitive load from ocular parameters. We calculated fixation rate, saccade rate and revisit sequences from eye gaze points. We also filtered the pupil dilation signal from the eye tracker using a low pass filter. The algorithms to calculate these metrics are described in the following sections.

4.1 Fixation and saccade rate

We calculated fixation rate and saccade rate by detecting fixations and saccades from gaze direction data using the velocity threshold fixation identification method (I-VT) [29]. I-VT is a velocity-based method that separates fixation and saccade points based on their point-to-point velocities. I-VT then classifies each point as a fixation or saccade based on a simple velocity threshold. If the point's velocity is below the threshold, it becomes a fixation point, otherwise it becomes a saccade point. We then calculated fixation and saccade rate as the number of fixations and saccades per second [18]. We calculated velocity in terms of visual angle i.e., degrees per second in order to render gaze velocity independent of the image and screen resolutions. This calculation is based on the relationship between the eye position in 3D space in relation to the stimuli plane and the gaze positions on the stimuli plane. The angle is calculated by taking the direction vector of two consecutive sample gaze points. The angle is then divided by the time between the two samples to get the angular velocity. The velocity threshold parameter is set to $40^\circ/\text{sec}$ [27]. The pseudo code for the I-VT method is shown in Table 1.

Table 1: Pseudocode for the I-VT algorithm

1. Calculate the angle between two consecutive points.
2. Calculate angular velocity by dividing the angle with the time between the two sample points.
3. Label each point below velocity threshold as a fixation and others as a saccade.
4. Return fixations and saccades.

4.2 Revisit sequences

A sequence refers to an ordered collection of focused nodes without repetitions. For example, A-B-C is a sequence, but A-A-B-C-C-C is not a sequence, where A, B and C are focused nodes. Revisit sequences provide information about how many times a participant scanned through a sequence [28]. This metric allows us to examine graphs that were repeatedly observed. We investigated three types of revisit sequences – sequences of lengths 3, 4 and 5. We also analysed two parameters of revisit sequences: (i) number of unique sequence and (ii) total revisit sequences. Unique revisit sequence is the distinct sequence for one graph that repeats itself. Total revisit sequences calculate all repetitions of every unique sequence. For the sequence of length three, if repetition is more than 3, the sequence is valid. For the sequence of length four, if repetition is more than 2, the sequence is valid. We did not consider revisits of the sequence of length five as there were less revisits for graphs. Figure 4 shows two unique sequences of length 3.

S1: Temperature – Humidity – Smoke

S2: Smoke – Air – Light

The pseudo code for the revisit sequence is shown in Table 2.

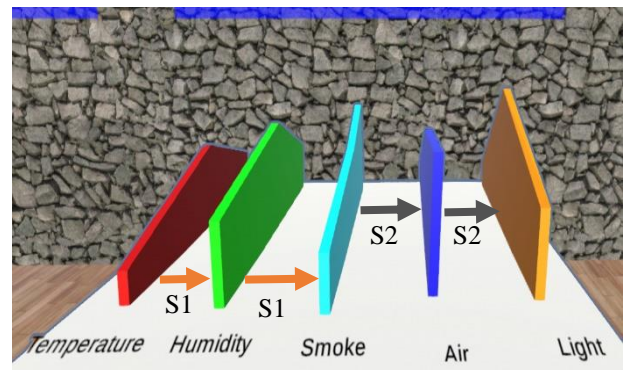


Figure 4: Two sequences of length 3

Table 2: Pseudocode for finding revisit sequences.

1. Find all nodes of the graph that participants were interested in and represent them into an array of sequential nodes.
2. Create a new sequence by the elimination of repetitive node placed in succession in a sequence.
3. Find unique sequences of length 3, 4 and 5 from the newly created sequence.
4. Calculate repetitions for each unique sequence.
5. Return number of unique sequences and the total number of revisits

4.3 Low pass filter of pupil (LPF)

Sudden hike in pupil dilation is related with change in cognitive load [20]. We divided the pupil dilation data into sections of 100 samples and subtracted mean from the raw data. We used a Butterworth lowpass filter with a cut off frequency of 5 Hz [40] and added the magnitude of the filtered data using a running window of size 1-sec with 70% overlap. This algorithm uses a conventional filtering technique in Digital Signal Processing (DSP), which uses time domain difference equations to filter the signal.

4.4 EEG data

We used EmotivBCI software [38] to monitor EEG signals and recorded data streams from EEG headset. The EmotivBCI software automatically calculates power signal for five EEG bands, we considered alpha, low beta, high beta and theta bands. We removed outlier from raw EEG data using inner fence.

5. Results

For all analyses, we calculated average values of parameters from all responses for all participants. We prepared tables of 6 columns corresponding to each type of graph and 17 rows corresponding to 17 participants. In all subsequent column graphs, the size of the column indicates average value while the error bar indicates standard deviation. We drew outline rectangles over columns which are statistically significantly different from each other.

We analysed the percentage of correct responses from the user for each chart. We analysed gaze-based metrics like fixation rate and saccade rate. We then calculated two parameters of revisit sequences and processed EEG data for further analysis. We analysed these parameters statistically for all participants across six charts. For statistical analysis we first undertook a Kolmogorov-Smirnov test for normality check. We then undertook Friedman test if data were not normally distributed.

The following subsections explain each parameter used for the analysis and results.

5.1 User responses

The percentage of correct answers for each chart is calculated as

$$\text{percentage} = \frac{\text{number of correct answers}}{\text{total number of questions}} * 100$$

Number of correct answers and total number of questions are calculated across all participants. We found that bar-size and bar-opacity are two charts that have highest percentage of correct answers. The comparison of percentage of correct answers across six charts is shown in Figure 5. We then carried out Wilcoxon Signed-Rank test between each pair of charts for correct answers. We found that BC is significantly different ($p < 0.05$) from BOR, SO, SS and AC is significantly different ($p < 0.05$) from SS. We also found that BO is significantly different ($p < 0.05$) from SO and SS.

5.2 Total task duration

We measured the average time taken to complete the task for each chart. We observed that bar-size has the lowest average time and bar-orientation has the highest. As this parameter does not include user responses it would be inappropriate to evaluate

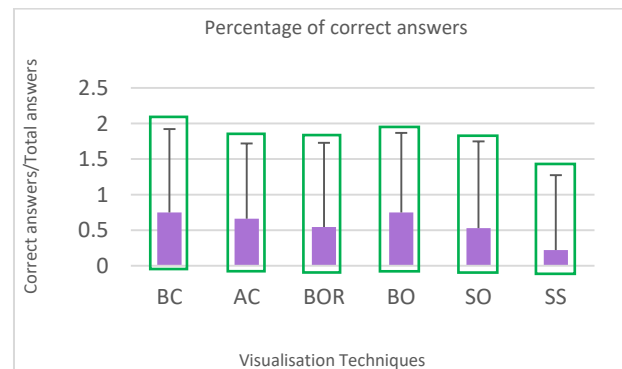


Figure 5: Percentage of correct answers

charts using only this parameter. For example, a chart with high task duration might perform better in user responses. The best-case scenario would be a high percentage of correct answers and low task duration. To mitigate this issue, we considered correct user responses along with total task duration. We refer this parameter as accuracy per unit time (APT) and is calculated as

$$\text{APT} = \frac{\text{number of correct answers}}{\text{total task duration}}$$

We found that APT of bar-size is the highest and shape-size is the lowest as depicted by Figure 6. We further undertook Friedman test for the average task duration of each participant. We found significant difference between means of charts (Chi square (5) = 15.354, $p < 0.05$). We then carried out Wilcoxon Signed-Rank test between each pair of charts. We

found BC and SS are significantly different from AC and BOR.

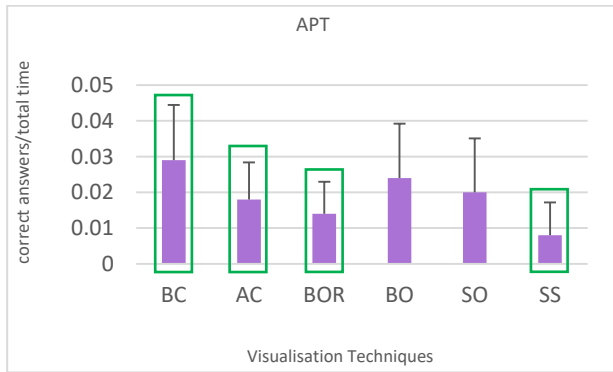


Figure 6: APT across all charts

5.3 Fixation and saccade rate

We calculated fixation and saccade rate for all participants across six charts. Bar-opacity has the lowest fixation rate but highest saccade rate. Bar-size has the highest fixation rate and area chart has the lowest saccade rate. Fixation and saccade rate would give information about total fixations during the task which includes movement of participant around the scene and answering questions. To investigate how long user focused only on visualisation chart we analysed fixation and saccade rate on chart. Fixation and saccade rate across all charts are shown in Figure 7 and 8, respectively. Bar-brightness chart has the highest fixation and saccade rate, while bar-orientation chart has the lowest. We then undertook Friedman test for the fixation and saccade rate of each participant during the entire task. We found significant difference between means of charts for fixation rate (Chi square (5) = 12.714, $p < 0.05$) and saccade rate (Chi square (5) = 14.214, $p < 0.05$). We then carried out Wilcoxon Signed-Rank test between each pair of charts for fixation and saccade rate. We found that BC and BO are significantly different ($p < 0.05$) from AC and BOR for fixation rate. We further noticed that BO is significantly different ($p < 0.05$) from BC, AC, BOR and SS.

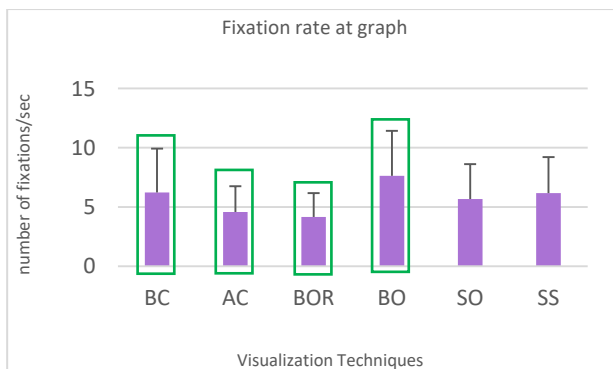


Figure 7: Fixation rate across all charts

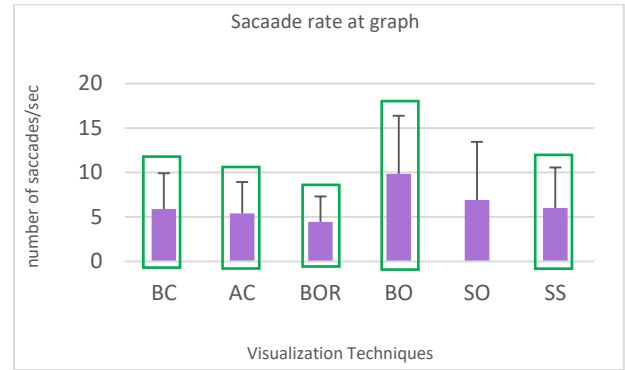


Figure 8: Saccade rate across all charts

5.4 Revisit sequences

Parameters of revisit sequences that we analysed are the number of unique sequences and the total number of revisits. A high number of unique sequences and total revisits would signify more combinations and repetitions. This would denote that participant was repeatedly scanning and focusing on the chart. We found that the bar-size chart has the lowest average unique sequences for sequences of length three and four while for sequences of length five shape-opacity chart has the lowest value. The bar-size chart also has the lowest total revisits for sequences of length three and four. Figures 9 and 10 show the number of unique sequences and total revisits for sequences of length three across all charts. We undertook Wilcoxon Signed-Rank test between each pair of charts for unique sequences and total revisits and did get significant difference ($p > 0.05$).

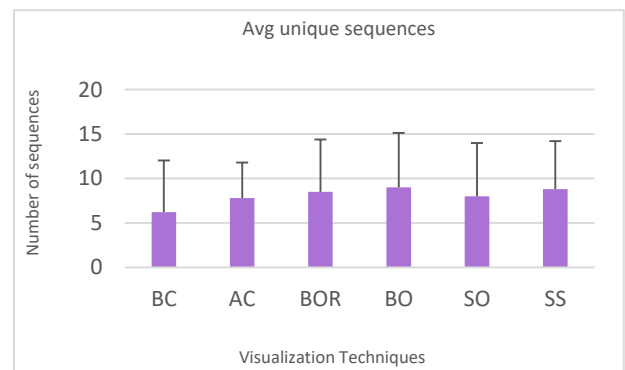


Figure 9: Unique sequences of length three sequences

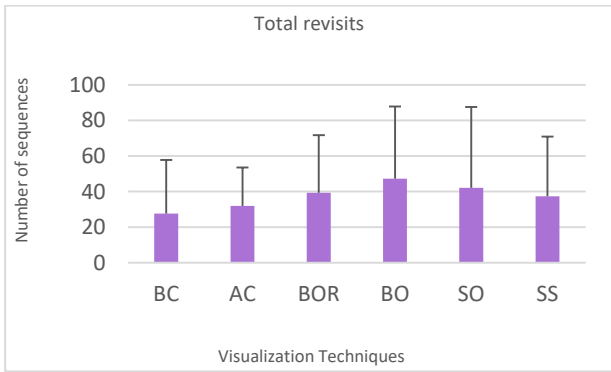


Figure 10: Total revisits of length three sequences

5.5 Analysis of pupil dilation

We undertook Friedman test on the output of LPF of the left and right pupil across all charts and found no significant difference ($p > 0.05$) between the means of charts. Furthermore, we completed the Wilcoxon Signed-Rank test between each pair of charts and found no significant difference. We observed that pupil dilation ranges from 2.75 mm to 6.68 mm.

5.6 EEG data analysis

A Friedman test was undertaken on alpha, theta, low beta (Figure 11), and high beta bands of EEG. We did not get significant difference for any EEG band. We then undertook the Wilcoxon Signed-Rank test between each pair of charts for four EEG bands.

1. Alpha band: We got significant difference ($p < 0.05$) between bar-size chart and area chart.
2. Theta band: We observed that bar-size chart is significantly different ($p < 0.05$) from area chart and bar-opacity chart.
3. Low beta band: We observed that bar-size chart is significantly different ($p < 0.05$) from area chart and bar-opacity chart. We got significant difference ($p < 0.05$) between bar-orientation and bar-opacity charts.

We found that bar-size chart is significantly different ($p < 0.05$) from the area chart in alpha, theta and low beta bands of EEG. We did not get any significant difference in the high beta band.

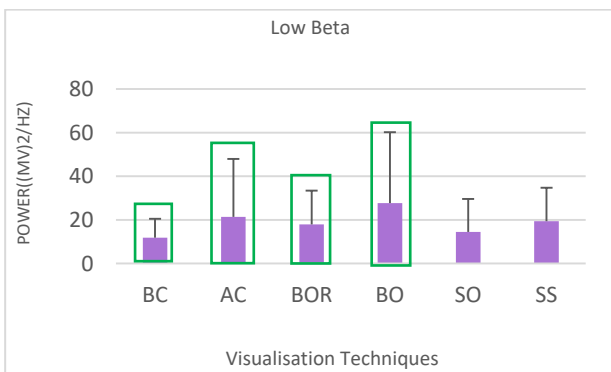


Figure 11: Average Low beta

5.7 Z-axis analysis

To analyse the effect of the 3rd dimension on participants, we separately investigated coordinates of gaze points. It would help us identify the impact of three axes on saccadic eye movements. We have considered all consecutive gaze points that form saccades. We calculated the absolute differences of coordinates between every two successive points. This calculation is based on L1 norm, which is the sum of the absolute differences of coordinates between two points. For example, if points $P1: \langle x1, y1, z1 \rangle$ and $P2: \langle x2, y2, z2 \rangle$ form a saccade, then the absolute differences of their coordinates are $|x1-x2|$, $|y1-y2|$, $|z1-z2|$. We then undertook the Friedman test on the computed absolute differences for every chart. We found that the absolute differences of coordinates are significantly different ($p < 0.05$) for all charts (Table 3). Furthermore, we undertook the Wilcoxon Signed-Rank test between each pair of coordinates for six charts. We found that the x-axis and z-axis are significantly different from the y-axis for all charts. We also analysed the movement of saccades along three axes. We calculated the average distance covered along the three axes during saccadic eye movement.

Table 3: Friedman test on differences of axes.

Bar size	Chi square (2) = 25.765, $p < 0.05$
Area chart	Chi square (2) = 22.706, $p < 0.05$
Bar orientation	Chi square (2) = 25.529, $p < 0.05$
Bar opacity	Chi square (2) = 20.235, $p < 0.05$
Shape opacity	Chi square (2) = 20.588, $p < 0.05$
Shape size	Chi square (2) = 20.588, $p < 0.05$

Figure 12 shows average distance of bar chart during saccade movement along all three axes. The distances are normalized from 0 to 1.

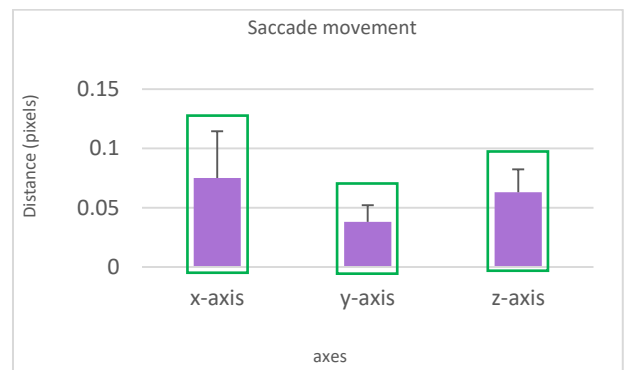


Figure 12: Average distance of bar chart

5.8 Comparisons of visual variables

As mentioned in Section 1, we have considered five visual variables in our study. Variable size, opacity, and orientation represent numerical data, while colour and shape depict nominal data. We investigated variables for each data type as

discussed in the sub-section below. We compared three parameters (APT, fixation rate and saccade rate) of each variable. We also compared revisit sequences between variables.

5.8.1. Visual variables for nominal data

We divided variables representing nominal data into following two categories -

- **Category1:** Nominal data is represented by colour.
- **Category2:** Nominal data is represented by both colour and shape.

Bar-Size, Bar-Orientation and Bar-Opacity charts fall under category1, while Shape-Size and Shape-Opacity charts fall under category2. We calculated the average value of three parameters for three charts in category1 and two charts in category2. We observed a difference in user performance between category1 and category2. APT is higher for category1 than category2, while fixation and saccade rate is lower for category2. The number of revisits is lower for category1 in the sequence of length 3 and 5 but higher in length 4.

5.8.2. Visual variables for numerical data

We divided variables representing numerical data into following three categories –

- **Category1:** Numerical data is represented by size.
- **Category2:** Numerical data is represented by orientation.
- **Category3:** Numerical data is represented by opacity.

Bar-Size and Shape-Size charts fall under category1, Bar-Opacity and Shape-Opacity charts fall under category3, while Bar-Orientation is a category2 chart. The average value of three parameters for charts in category1 and category2 are computed. We then compared these parameters among the charts of three categories and noticed a difference in user performance between all three groups. The fixation and saccade rate are lower for category2 than the other two categories. However, in terms of task duration, accuracy is higher for category1. The number of sequences is higher in category3 for sequences of length 3, 4 and 5.

6. Discussion

Our results showed that accuracy per unit time is higher for size and colour than other variables. We further observed that variable size and colour have a smaller number of fixations, saccades, and total revisits. Furthermore, our results showed a difference in cognitive load between size, opacity, and brightness. We can infer from these results that the cognitive load of participants is less when size is used to represent numerical data and colour is used to depict nominal data. In addition, from

results of our analysis, we noticed that cognitive load while using a bar chart is less to an area chart. Finally, we looked back at four questions that we had raised in Section 1 –

Q1: Which 3D graph is best in terms of correct data interpretation?

We observed from Figure 5 that both bar-opacity and bar-size are similar in terms of correct data interpretation. We then noticed that bar-size's accuracy per unit time is higher than other charts and requires least number of revisits. We can infer from these results that bar-size chart is best in terms of correct data interpretation.

Q2: Which visual variables(s) is (are) easier to interpret than others?

We found that colour makes it easier to interpret nominal data as compared to shape. Performance of variable colour is higher in two gaze-based metrics and task duration as compared to shape in terms of accuracy. The size variable reduces the time required for processing numerical data as compared to the other two variables. However, size is similar to orientation for the other two ocular parameters (fixation and saccade rates). The size variable also performs favourably in terms of the count of revisit sequences. In addition, from our results we observed that opacity is worst in terms of correct data interpretation among three variables. We further observed that bar chart has lower cognitive load than area chart.

Q3: Does 3rd dimension add value to the visualisation?

We also observed that the addition of the 3rd dimension to the visualisation affects the performance of participants. We noticed that the movement of saccades along the z-axis is more than the movement along y-axis but less than the movement along x-axis, as shown in Figure 12. Moreover, the movement of saccades along axes were significantly different, as described in Table 6. This conveys that the movement along all axes are important and offers new information to participants.

Q4: Are there differences among graph types with respect to - ocular parameters, and cognitive load while interpreting graphs.

Notably, significant differences were observed among certain chart types with respect to ocular parameters. For example, bar-opacity and bar-orientation are different in terms of the fixation rate, as shown in Table 4. Similarly, significant differences were noticed among six pairs of charts concerning cognitive load. However, we found significant difference only between area chart and bar-size in all the three bands measured.

Beta band, especially in the sensory motor areas, are related to motor movements. A high value of power in the low beta band signifies low cognitive

load [41]. We observed that bar-size has the highest value and bar-opacity has the lowest value in the low beta band. It indicates that bar-size chart is incurring less motor action and cognitive load.

Limitations and Future Work

This study evaluated six different graph types involving five different visual variables. The study design and analysis did not investigate interaction effects among chart types and visual variables. We were limited by time and resource in terms of availability of participants and a repeated measure design with 2 types of graphs and five variables would increase duration of the experiment as well as required more participants than reported presently. A future work will limit the number of variables and analyse interaction effect.

Our sampling strategy did not measure participants' familiarity with different 2D graphs and the bar graph may found to be easier to interpret as participants were more familiar to it than area graph. However, it may be noted that our study involved three different types of bar graphs and the results related to visual variables are still useful for a single type of graph.

In the study design, we utilized all three axes to display data points and their values and users found to use both saccades and vergance eye gaze movements to browse through graphs. Future work will separately analyse saccades and vergance and report their proportions while interpreting 3D graphs.

For EEG analysis, we used a low-cost EEG headset and so did not analyse high frequency signals like Gamma band, future work will investigate ergonomic issues involving donning both a VR Headset and EEG cap and try to use an EEG device with more electrodes than the Emotiv Insight model.

Application

We have developed a VR model of a smart factory and set up visualization graphics at the locations of IoT nodes to embed real-time sensor readings on the virtual layout (Figure 13). We used the Unity 3D game engine and its modelling tool, Probuilder. The twin served as a three-dimensional illustration of the physical space whose dimensions were accurately mapped to the twin. Furthermore, the furniture and other objects in the physical space were also replicated in the virtual world. To improve the virtual environment's photorealism, baked global illumination was used, which entails computing the lighting behaviour and characteristics beforehand and storing them as texture files; this technique also reduces the computational load present in real-time global illumination. Additionally, Physically Based Materials or PBR were used as they physically simulate real-life materials' properties such that they accurately reflect the flow of light and thereby achieve photorealism. We deployed the twin on a Virtual Reality (VR) setup, specifically, the HTC Vive

Pro Eye, since VR allows for immersive and interactive virtual walkthroughs. Users can browse through the virtual set up using 3D glass and as they touch any of the visualization, it provides both visual and haptic feedback based on sensor readings. We integrated ambient light sensor (BH1750) and, temperature and humidity sensor (DHT22) to show real-time visualization of data stream(s) in VR setup. Both sensors provide digital output. The BH1750 Sensor has a built-in 16-bit A2D converter and output unit is lux. The DHT22 sensor provides temperature in celcius and humidity as relative percentage. Sensors are interfaced to the VR machine through their respective wireless module(s). After establishing a peer-to-peer connection, individual wireless module communicates with VR machine using UDP protocol at a frequency of 1 Hz. A video demonstration of the system can be found at <https://youtu.be/FX8zfQE5GF8>

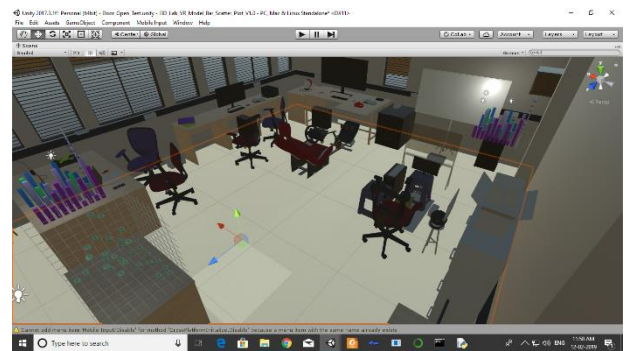


Figure 13. 3D Sensor Dashboard in a Digital Twin

7. Conclusion

This paper compared six different types of 3D graphs with respect to users' subjective and objective feedback. We analysed speed-accuracy trade off in users' response with respect to representative graph interpretation tasks. We also recorded and analysed ocular parameters and EEG to investigate eye gaze movement patterns and cognitive load while interacting with 3D graphs. A bar chart with different size of columns for different values of data points found out to generate most accurate response and least cognitive load among users.

8. References

1. Isenberg, T., Isenberg, P., Chen, J., Sedlmair, M., & Möller, T. (2013). A systematic review on the practice of evaluating visualization. *IEEE Transactions on Visualization and Computer Graphics*, 19(12), 2818-2827.
2. Steichen, B., Wu, M. M., Toker, D., Conati, C., & Carenini, G. (2014, July). Te, Te, Hi, Hi: Eye gaze sequence analysis for informing user-

- adaptive information visualizations. In *International Conference on User Modeling, Adaptation, and Personalization* (pp. 183-194). Springer, Cham.
3. Arjun, S. (2018, July). Personalizing data visualization and interaction. In *Adjunct Publication of the 26th Conference on User Modeling, Adaptation and Personalization* (pp. 199-202).
 4. Huang, Y. J., Fujiwara, T., Lin, Y. X., Lin, W. C., & Ma, K. L. (2017, April). A gesture system for graph visualization in virtual reality environments. In *2017 IEEE Pacific Visualization Symposium (PacificVis)* (pp. 41-45). IEEE.
 5. Capece, N., Erra, U., & Grippa, J. (2018, July). Graphvr: A virtual reality tool for the exploration of graphs with htc vive system. In *2018 22nd international conference information visualisation (iv)* (pp. 448-453). IEEE.
 6. Erra, U., Malandrino, D., & Pepe, L. (2019). Virtual reality interfaces for interacting with three-dimensional graphs. *International Journal of Human-Computer Interaction*, 35(1), 75-88.
 7. Sullivan, P. A. (2016). Graph-based data visualization in virtual reality: a comparison of user experiences.
 8. Ware, C., & Franck, G. (1994, October). Viewing a graph in a virtual reality display is three times as good as a 2D diagram. In *Proceedings of 1994 IEEE Symposium on Visual Languages* (pp. 182-183). IEEE.
 9. Ward, M. O., Grinstein, G., & Keim, D. (2010). *Interactive data visualization: foundations, techniques, and applications*. CRC Press.
 10. Andrews, K. (2006, May). Evaluating information visualisations. In *Proceedings of the 2006 AVI workshop on BEyond time and errors: novel evaluation methods for information visualization* (pp. 1-5).
 11. Carpendale, S. (2008). Evaluating information visualizations. In *Information visualization* (pp. 19-45). Springer, Berlin, Heidelberg.
 12. Chen, C., & Czerwinski, M. P. (2000). Empirical evaluation of information visualizations: an introduction. *International journal of human-computer studies*, 53(5), 631-635.
 13. Livingston, M. A., Decker, J. W., & Ai, Z. (2012). Evaluation of multivariate visualization on a multivariate task. *IEEE transactions on visualization and computer graphics*, 18(12), 2114-2121.
 14. Amar, R., Eagan, J., Stasko, J.: Low-Level Components of Analytic Activity in Information Visualization. In: *Proc. of 2005 Symp. on Information Visualization*, pp. 15–21 (2005)
 15. Conati, C., Maclaren, H.: Exploring the role of individual differences in information visualization. In: *Proc. of the Working Conf. on Advanced Visual Interfaces*, pp. 199–206 (2008)
 16. Velez, M.C., Silver, D., Tremaine, M.: Understanding visualization through spatial ability differences. In: *IEEE Visualization, VIS 2005*, pp. 511–518 (2005)
 17. Toker, D., Conati, C., Carenini, G., Haraty, M.: Towards adaptive information visualization: On the influence of user characteristics. In: Masthoff, J., Mobasher, B., Desmarais, M.C., Nkambou, R. (eds.) *UMAP 2012*. LNCS, vol. 7379, pp. 274–285. Springer, Heidelberg (2012)
 18. Prabhakar, G., Mukhopadhyay, A., Murthy, L., Modiksha, M., Sachin, D., & Biswas, P. (2020). Cognitive load estimation using ocular parameters in automotive. *Transportation Engineering*, 2, 100008.
 19. Palinko, O., Kun, A. L., Shyrokov, A., & Heeman, P. (2010, March). Estimating cognitive load using remote eye tracking in a driving simulator. In *Proceedings of the 2010 symposium on eye-tracking research & applications* (pp. 141-144).
 20. Marshall, S. P. (2002, September). The index of cognitive activity: Measuring cognitive workload. In *Proceedings of the IEEE 7th conference on Human Factors and Power Plants* (pp. 7-7). IEEE.
 21. Gavvas, R., Chatterjee, D., & Sinha, A. (2017, October). Estimation of cognitive load based on the pupil size dilation. In *2017 IEEE International Conference on Systems, Man, and Cybernetics (SMC)* (pp. 1499-1504). IEEE.
 22. Duchowski, A. T., Krejtz, K., Krejtz, I., Biele, C., Niedzielska, A., Kiefer, P., ... & Giannopoulos, I. (2018, April). The index of pupillary activity: Measuring cognitive load vis-à-vis task difficulty with pupil oscillation. In *Proceedings of the 2018 CHI Conference on Human Factors in Computing Systems* (pp. 1-13).
 23. Biswas, P., & Prabhakar, G. (2018). Detecting drivers' cognitive load from saccadic intrusion. *Transportation research part F: traffic psychology and behaviour*, 54, 63-78.
 24. Goldberg, J., Helfman, J.: Eye tracking for visualization evaluation: reading values on linear versus radial graphs. *Inf. Vis.* 10, 182–195 (2011)
 25. Iqbal, S.T., Bailey, B.P.: Using eye gaze patterns to identify user tasks. Presented at the The Grace Hopper Celebration of Women in Computing (2004)
 26. Toker, D., Conati, C., Steichen, B., Carenini, G.: Individual user characteristics and information visualization: connecting the dots through eye tracking. In: *Proceedings of the SIGCHI Conference on Human Factors in Computing Systems*, pp. 295–304 (2013)
 27. Olsen, A., & Matos, R. (2012, March). Identifying parameter values for an I-VT fixation filter suitable for handling data sampled with various sampling frequencies. In *proceedings of the symposium on Eye tracking research and applications* (pp. 317-320)

28. Farnsworth, B. (2021). 10 Most Used Eye Tracking Metrics and Terms - iMotions. Retrieved 24 April 2021, from <https://imotions.com/blog/10-terms-metrics-eye-tracking/#revisits>
29. Salvucci, D. D., & Goldberg, J. H. (2000, November). Identifying fixations and saccades in eye-tracking protocols. In Proceedings of the 2000 symposium on Eye tracking research & applications (pp. 71-78).
30. Ziemkiewicz, C., Crouser, R. J., Yauilla, A. R., Su, S. L., Ribarsky, W., & Chang, R. (2011, October). How locus of control influences compatibility with visualization style. In 2011 IEEE Conference on Visual Analytics Science and Technology (VAST) (pp. 81-90). IEEE.
31. Green, T. M., & Fisher, B. (2010, October). Towards the personal equation of interaction: The impact of personality factors on visual analytics interface interaction. In *2010 IEEE Symposium on Visual Analytics Science and Technology* (pp. 203-210). IEEE.
32. Peck, E. M. M., Yuksel, B. F., Ottley, A., Jacob, R. J., & Chang, R. (2013, April). Using fNIRS brain sensing to evaluate information visualization interfaces. In Proceedings of the SIGCHI Conference on Human Factors in Computing Systems (pp. 473-482).
33. Ware, C., & Mitchell, P. (2008). Visualizing graphs in three dimensions. *ACM Transactions on Applied Perception (TAP)*, 5(1), 1-15.
34. Fisher III, S. H., Dempsey, J. V., & Marousky, R. T. (1997). Data visualization: Preference and use of two-dimensional and three-dimensional graphs. *Social Science Computer Review*, 15(3), 256-263.
35. Garlandini, S., & Fabrikant, S. I. (2009, September). Evaluating the effectiveness and efficiency of visual variables for geographic information visualization. In *International Conference on Spatial Information Theory* (pp. 195-211). Springer, Berlin, Heidelberg.
36. Roth, R. E. (2017, March 6). Visual Variables. <https://onlinelibrary.wiley.com/doi/abs/10.1002/9781118786352.wbieg0761>
37. The professional-grade VR headset | VIVE Pro United States. Vive.com. (2021). Retrieved 7 May 2021, from <https://www.vive.com/us/product/vive-pro/>.
38. Insight Brainwear® 5 Channel Wireless EEG Headset | EMOTIV. EMOTIV. (2021). Retrieved 7 May 2021, from <https://www.emotiv.com/insight/>.
39. Biswas P and Robinson P, Evaluating the design of inclusive interfaces by simulation, Proceedings of the ACM International Conference on Intelligent User Interfaces (IUI) 2010
40. Onorati, F., Barbieri, R., Mauri, M., Russo, V., & Mainardi, L. (2013, July). Reconstruction and analysis of the pupil dilation signal: Application to a psychophysiological affective protocol. In 2013 35th Annual International Conference of the IEEE Engineering in Medicine and Biology Society (EMBC) (pp. 5-8). IEEE.
41. 5 Types of Brain Waves Frequencies: Gamma, Beta, Alpha, Theta, Delta - Mental Health Daily. Mental Health Daily. (2021). Retrieved 10 May 2021, from <https://mentalhealthdaily.com/2014/04/15/5-types-of-brain-waves-frequencies-gamma-beta-alpha-theta-delta/>.
42. Drogemuller, A., Cunningham, A., Walsh, J., Cordeil, M., Ross, W., & Thomas, B. (2018, October). Evaluating navigation techniques for 3d graph visualizations in virtual reality. In 2018 International Symposium on Big Data Visual and Immersive Analytics (BDVA) (pp. 1-10). IEEE.